# Analysis of Membrane-Binding Properties of Dermaseptin Analogues: Relationships between Binding and Cytotoxicity†

Leonid Gaidukov, Alexander Fish, and Amram Mor*

*The Laboratory for Antimicrobial Peptides Investigation, Department of Food Engineering and Biotechnology, Technion−Israel Institute of Technology, Haifa, Israel*

*Received April 1, 2003; Revised Manuscript Received August 14, 2003*

ABSTRACT: To understand relationships between membrane-binding properties of cytolytic peptides and resulting cytotoxicity, we investigated interactions of dermaseptin analogues with model bilayers by means of surface plasmon resonance. First, we tested the system by comparing two native dermaseptins, S1 and S4, whose binding properties were previously characterized in different experimental systems. Validation experiments revealed deviations from the one-to-one interaction model and indicated the binding to proceed by a two-stage mechanism. By calculation of apparent affinity constants and individual affinities for both steps of the interaction, the biosensor technology was able to distinguish between surface-bound peptides that subsequently penetrated into the bilayer and peptides that remained essentially superficially bound. This data interpretation was sustained after analysis of a series of dermaseptin S4 derivatives whose binding data were compared with cytotoxicity, revealing cytolytic activity to correlate mainly with insertion affinity. The data indicate that the potency of highly cytolytic peptides such as $K_4K_{20}$-S4 is not due to the highest membrane adhesion affinity but to the highest propensity for the inserted state. Similarly, truncated derivatives of 16, 13, and 10 residues showed a progressive reduction in cytotoxicity that best correlated with progressive reduction in insertion affinity. Support for the adhesion versus inserted states was provided by proteolytic experiments with RBC-bound peptides that demonstrated $K_4K_{20}$-S4 to be protected from enzymatic cleavage, unlike its 13-mer derivative. Overall, using the two-stage model proved instrumental in investigating membrane-binding properties of antimicrobial peptides and capable of explaining the cytolytic properties of closely related analogues.

After a half century of virtually complete control over microbial infections, antibiotic resistance has become of great concern. Resistance has developed to almost all antimicrobial drugs, and bacterial strains resistant to all available antibacterial agents have been identified (*1*, *2*). The development of new classes of antibiotics is thus becoming increasingly important. As possible candidates, the ubiquitously produced in nature cationic antimicrobial peptides (*3*, *4*) were shown to escape some of the mechanisms involved in multidrug resistance and are thus attracting increasing research and clinical interest (*5*). Through extensive studies of these peptides during the past decades, it has become indisputably evident that they represent an essential component of the innate defense mechanisms (*6*−*9*).

Antimicrobial peptides often exhibit potent activity against a wide spectrum of microorganisms at concentrations that are nontoxic to normal eukaryotic cells. The molecular basis for this selectivity is ill-defined but is believed to result from differences in lipid composition of target versus nontarget cells, such as membrane fluidity, high negative charge density, and possession, by the peptide-susceptible organism, of a large negative transmembrane electrical potential (*10*, *11*). These differences seem to be responsible for the preferred accumulation of antimicrobial peptides on microbial membranes, inducing their disruption. Numerous studies demonstrated that the peptides' physicochemical properties, including amphipathy, positive charge content, and hydrophobicity, are the main factors affecting membrane-lytic activity (*11*−*14*). The cytoplasmic membrane was proposed as one of the ultimate targets of antimicrobial peptides (*6*). Being cationic, they are able to interact electrostatically with the negatively charged headgroups of bacterial phospholipids and then insert into the membrane bilayer. Membrane lysis is proposed to proceed via numerous mechanisms involving membrane perforation/disruption/solubilization (*15*, *16*). For instance, pore formation was proposed for the hemolytic peptide melittin (*17*) whereas the mechanism of action of cecropin P1 was proposed to proceed by membrane disruption (*18*). Thus, although the precise mechanism of action remains to be better understood, the microbicidal effect is believed to result from the peptides' capacity to permeabilize the membrane of target cells. Indeed, most antimicrobial peptides provoke an increase in plasma membrane permeability, dissipate the transmembrane electrical potential (*19*−*23*), conduct ions across lipid bilayers (*24*), and display direct correlation between permeabilization ability and antimicrobial effect (*10*, *25*). It should be noted that other studies have indicated that certain antimicrobial peptides can translocate into the cytoplasm of prokaryotic (*26*) and eukaryotic cells (*27*−*29*), suggesting a role for these peptides against intracellular targets.

† This work is supported by the Israel Science Foundation (Grant 387/03).

* Corresponding author. Tel: +972 4 829 3340. Fax: +972 4 829 3399. E-mail: amor@tx.technion.ac.il.

10.1021/bi034514x CCC: $25.00 
Published on Web 10/14/2003

There is thus a clear need for improving our understanding of the modes of the peptides' interaction with the membrane of target cells and defining precisely how this would lead to cell death. In this respect, it was recently stipulated that, independently of the mechanism of membrane permeabilization, cationic antimicrobial peptides have two distinct states of binding: parallel to the membrane surface at low peptide-to-lipid ratios (surface state) and perpendicular to the plane of the bilayer at high peptide-to-lipid ratios (insertion state) (*30*−*32*). Accordingly, the action of antimicrobial peptides is affected by the transition from the surface to insertion state (*32*). This transition takes place at some threshold concentration of the membrane-bound peptide, which is roughly the same as the critical concentration required for cytotoxic activity, implying that peptide insertion into the membrane is responsible for cytotoxicity. In accordance with this model, microbicidal activity exhibits strong concentration dependence. At lower concentrations, the peptides are virtually inactive until a critical concentration is reached (*15*, *16*), suggesting that the active form of the peptide is an oligomer and that peptide self-assembly on the membrane surface can be a precursory condition for membrane-lytic activity.

The dermaseptins are a large family of linear cationic peptides (*33*−*35*) displaying cytolytic activity against a broad spectrum of pathogens. The cytolytic activity of members of this family is mediated by interactions of their amphipathic N-terminal domain with plasma membrane phospholipids (*14*, *36*−*44*). Unlike most natural dermaseptins, dermaseptin S4 is highly toxic to erythrocytes presumably mediated by intermonomer hydrophobic interactions leading to self-assembly in solution (*14*, *42*, *45*). Fluorescence-based studies using liposomes revealed dermaseptin S4 to partition into the lipid phase with a surface partition coefficient ($K_p$) of nearly $10^6$ $M^{-1}$ (Jimut Ghosh, private communications). Tampering with the composition of the hydrophobic terminal domains led to disassembly (*42*) and to improved antimicrobial properties both in vitro and in vivo (*46*, *47*). Recently, dermaseptin S4 and selected derivatives were investigated with respect to relations between physicochemical properties (composition, structure, and organization in solution) and interaction with target membranes (*14*). Surface plasmon resonance (SPR)[1] was used to study the peptides' lipid-binding behavior. Dermaseptin S4 and various derivatives were shown to bind to model-charged membranes with association affinity constants ($K_A$) in the range of $10^6-10^7$ $M^{-1}$. However, these calculations were based on the assumption that the binding process proceeds by simple association between the peptide and lipid. Recent reports on SPR binding analysis between magainin or melittin and lipid mono- and bilayer surfaces proposed that kinetic analysis with more complex models resulted in an improved fit (*48*, *49*). In this study, using dermaseptin analogues, we applied the SPR technology to bilayer surfaces in an attempt to improve our understanding of the relationships between membrane-binding properties and the hypothetical outcome: cytolytic activity.

[1] Abbreviations: PC, egg yolk L-α-phosphatidylcholine; PA, L-α-phosphatidic acid; PBS, phosphate-buffered saline; HPLC, high-performance liquid chromatography; RBC, red blood cells; SPR, surface plasmon resonance; SUV, small unilamellar vesicles; RU, resonance units.

## MATERIALS AND METHODS

*Peptides.* Peptides were synthesized by the solid-phase method as described (*14*), applying the Fmoc (9-fluorenylmethyloxycarbonyl) active ester chemistry on a fully automated, programmable Model 433A peptide synthesizer (Applied Biosystems). [4-(Hydroxymethyl)phenoxy]methyl−co-polystyrene−1% divinylbenzene resin (Wang resin) and 4-methylbenzhydrylamine resin (Novabiochem) were used to obtain free carboxyl or amidated peptides, respectively. After cleavage from the resin, the crude peptide was extracted with 30% acetonitrile in water and purified to chromatographic homogeneity in the range of 98% to >99% by reverse-phase HPLC (Alliance-Waters). HPLC runs were performed on a semipreparative C4 column (Vydac) using a linear gradient of acetonitrile in water (1%/min), both solvents containing 0.1% trifluoroacetic acid. The purified peptides were subjected to amino acid analysis and/or mass spectrometry in order to verify their composition. Peptides were stored as a lyophilized powder at −20 °C. Prior to being tested, fresh solutions were prepared in water, vortexed, sonicated, centrifuged, and then diluted in the appropriate medium. Buffers were prepared using distilled water (mQ, Millipore). All other reagents were of analytical grade.

*Liposome Preparation.* Egg yolk L-α-phosphatidylcholine and L-α-dipalmitoylphosphatidic acid were used to prepare liposomes. Small unilamellar vesicles (SUV) composed of phosphatidylcholine (PC) or phosphatidylcholine/phosphatidic acid (PC/PA, 1:1 molar ratio) were prepared in PBS by the extrusion method (*50*). Briefly, dry PC and PA were dissolved in EtOH or $CHCl_3$, respectively. The resultant solution of PC and an equimolar mixture of PC/PA were added to glass vials, and the solvents were evaporated under stream of nitrogen for at least 30 min. Dried lipids were then resuspended in PBS buffer at 0.5 mM total lipid concentration. The obtained suspension was vigorously vortexed, briefly sonicated, and passed (21 times) through 100 nm polycarbonate membranes in a LiposoFast-Basic extrusion apparatus (Avestin, Inc.) to give a translucent solution of vesicles with a mean diameter of 100 nm.

*Surface Plasmon Resonance (SPR) Analysis.* Peptide binding to phospholipid membranes was determined using the optical biosensor system (BIAcore 3000, Uppsala, Sweden) based on the principles of surface plasmon resonance (*51*). The sensor chip L1 (a carboxymethyldextran hydrogel derivatized with lipophilic alkyl chain anchors) designed to facilitate liposome-mediated hydrophobic adsorption (*52*) was used to prepare a lipid bilayer as described (*14*). Briefly, after the chip was washed with octyl glucoside (40 mM), the liposomes (0.5 mM) were injected over the chip surface at a flow rate of 2 μL/min at 25 °C to allow fusion with the hydrophobic surface of the chip. Irregular and loosely bound structures such as multiple lipid layers and partially fused liposomes were washed away by a brief injection of NaOH (50 mM) at a high flow rate (100 μL/min). Bovine serum albumin (BSA) was used to assess the degree of surface coverage. About 5000 resonance units (RU) of lipid were immobilized under these conditions, corresponding to a surface lipid density of 4.6 ng/mm$^2$ (*53*). The binding assay was performed by injecting peptide solutions in PBS at five different concentrations (typically 0.5−1.5 or 10 μM, respectively, for native peptides and derivatives)

in duplicates at a flow rate of 5 $\mu$L/min at 25 °C. Surface regeneration between consecutive binding cycles included a sequential injection of NaOH (50 mM) and HCl (50 mM). A run time of 3 mins was necessary for complete regeneration of the phospholipid membrane.

*Data Analysis.* (*1) Linearization Analysis*. The method involves a linear transformation of the binding data to determine kinetic parameters (*54*) and is intended for the interactions that follow a simple bimolecular association (Langmuir kinetics) between peptide P and lipid L:

$$P + L \leftrightarrow PL$$

The corresponding differential rate equation for this reaction is

$$dR/dt = k_a C_A(R_{max} - R) - k_d R$$

where $R$ is the response in RU that corresponds to the concentration of the molecular complex formed, $C_A$ is the concentration of the peptide, $R_{max}$ is the maximum response (corresponds to the total concentration of immobilized lipids), and $k_a$ and $k_d$ are the association and dissociation rate constants, respectively.

In the case of a simple bimolecular interaction the association rate ($k_a$) can be determined from the slope of the response signal change (d$R$/d$t$) versus the response ($R$) or, in logarithmic terms, ln(d$R$/d$t$) versus time (s). The dissociation rate ($k_d$) can also be determined via linearizing the dissociation phase by plotting ln($R_0/R$) versus time (s) ($R_0$ is the response at time zero and $R$ is the response at time $t$). Linear slopes should be observed in the case of a simple bimolecular interaction. However, nonlinear slopes reflect either mass transfer limitations or complex interactions, and the rate constants cannot be accurately determined (*54*). The shape of the ln(d$R$/d$t$) versus $t$ plot provides information on the nature of the interaction involved; i.e., the plot is linear for the 1:1 interaction, and it has a convex form for the 1:1 interaction limited by mass transfer and has a concave form for complex interactions [manufacturer's instructions (*64*)].

*(2) Two-Stage Model*. Association and dissociation rate constants are calculated using BIAevaluation 3.0 software (Biacore AB) by nonlinear fitting of the primary sensorgram data with algorithms for numerical integration (*55*) and global analysis (*56*). To compensate for the variation of baseline level between the injection cycles, the maximum response ($R_{max}$) was set to a local parameter, i.e., determined separately for each sensorgram. For reasons detailed below, the sensorgrams were routinely analyzed according to a two-stage binding model (conformational change) which, in terms of peptide−lipid interaction, may correspond to stage 1, peptide (P) binding to lipids (L) to give PL, followed by stage 2, the complex PL changing to PL* which cannot dissociate directly to P + L and which may correspond to insertion of the peptide into the membrane bilayer:

$$P + L \leftrightarrow PL \leftrightarrow PL^*$$

$$[PL] = R_1$$

$$[PL^*] = R_2$$

Table 1: Sequence of the Dermaseptin Peptides Investigated

| Peptide | Amino acid sequence[a] |
|---|---|
| S1 | ALWKTMLKKLGTMALHAGKAALGAAADTISQGTQ |
| S4 | ALWMTLLKKVLKAAAKAALNAVLVGANA |
| $K_4K_{20}$-S4 | ---K----------K-------- |
| $K_4$-S4(1-16)a | ---K----------$_{NH2}$ |
| $K_4$-S4(1-13)a | ---K---------$_{NH2}$ |
| $K_4$-S4(1-10)a | ---K------$_{NH2}$ |

[a] The amino acid sequence is in the standard one-letter code; a = amide. Dashes represent amino acids identical to those in S4.

The rate constants are derived from the differential equations (*55*):

$$dR_1/dt = k_{a1}C_A(R_{max} - R_1 - R_2) - k_{d1}R_1 - k_{a2}R_1 + k_{d2}R_2$$

$$dR_2/dt = k_{a2}R_1 - k_{d2}R_2$$

$$\text{total response: } R_1 + R_2$$

$K_{A1}(k_{a1}/k_{d1})$ and $K_{A2}(k_{a2}/k_{d2})$ are the association affinity constants of the first and second stages of the reaction, respectively. Their product ($K_{A1} \times K_{A2}$) yields the association affinity constant $K_{apparent}$.

*Cytolytic Activity.* Membrane-lytic activity was assessed with human red blood cells (RBC) and *Leishmania major* promastigotes as described (*14*).

*Susceptibility of Membrane-Bound Peptides to Proteolysis.* RBC-bound peptides were submitted to proteolytic treatment, then extracted, and analyzed by HPLC basically as described (*46*) with the following variation. Human RBC were rinsed in PBS by centrifugation, and then 10 $\mu$L of packed cells was exposed to 10 $\mu$M $K_4K_{20}$-S4 (28.6 $\mu$g) or $K_4$-S4(1−13)a (15.1 $\mu$g) in 1 mL of PBS. After an incubation period (15 min under shaking at 37 °C) unbound peptide was washed away by repeated (3×) centrifugation, and cell pellets were resuspended in 1 mL of PBS alone or PBS containing 1 unit of proteinase K for 15 min incubation under shaking at 37 °C, including several short vortex/sonication cycles to optimize enzyme contact with the cells. Incubation was followed by a rinse cycle, and then the membrane-bound peptides were extracted from the resulting cell pellets using 0.2 mL of octyl glucoside (1%, 2 min, 25 °C) and analyzed by reverse-phase HPLC.

## RESULTS

Toward better understanding the modes of interaction between peptides and phospholipid membranes, dermaseptin S1, dermaseptin S4, and a series of derivatives were generated (the peptide sequences are listed in Table 1). Peptide purity was in the range of 95% to >99% as determined by analytical HPLC; their identity was confirmed by mass spectrometry and amino acid analysis (data not shown).

The suitability of Biacore methodology for the analysis of peptide−membrane interaction was initially assessed using the native peptides S1 and S4, whose binding properties to phospholipid vesicles of different compositions were previ-

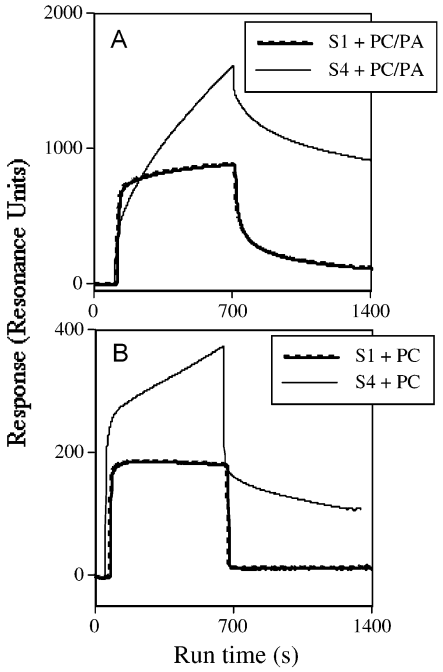


FIGURE 1: Overlay of sensorgrams for the binding of dermaseptin analogues to bilayered membranes immobilized onto the L1 chip. The plots depict the interaction kinetics of dermaseptin S1 (dashed line) and S4 (solid line) at the highest peptide concentration tested (1.5 $\mu$M) in PBS at 25 °C. Membranes are composed respectively with PC/PA (1:1) in panel A and with PC alone in panel B. Each sensorgram represents an average curve of two injections.

ously characterized (*19*, *45*). The validation study was followed by detailed investigation of dermaseptin S4 derivative binding and hemolytic properties.

*Validation of SPR Methodology.* To determine the peptide lipophilic properties, small unilamellar vesicles were adsorbed onto the sensor chip L1 to form a supported lipid bilayer that chemically and physically resembles the surface of a cell membrane. Typical binding profiles of the peptides to zwitterionic (PC) and acidic (PC/PA) membranes are portrayed in Figure 1 for the highest concentrations tested (1.5 $\mu$M). The binding levels of S4 to both PC/PA and PC increased as a function of peptide concentrations (data not shown), which is indicative of specific interaction between the peptides and the phospholipid membranes. A similar pattern was observed for binding of S1 to PC/PA. However, there was no detectable binding between S1 and the PC membrane up to 1.5 $\mu$M, indicating that the affinity of S1 to the PC bilayer is too low to be determined under the concentration range used. Comparison of the binding profiles of S1 and S4 to the PC/PA bilayer shows that the peptides differ in their affinity, as revealed by the binding levels, as well as in the kinetics of the interaction (the rate of response signal change for association and dissociation phases). Dermaseptin S1 associated with the charged membrane in fast kinetics readily reaching steady-state level, whereas the binding of S4 proceeded with slower kinetics, but its binding capacity was significantly larger. The slower dissociation rate too indicated that S4 binds more avidly to the membrane. Moreover, S4 continued to accumulate on the membrane surface during the entire injection phase without reaching the equilibrium level. The binding curves did not reach equilibrium during sample injection even after increased injection times (not shown). This behavior may be related to the complex mode of interpeptide interaction of dermaseptin S4 (i.e., peptide self-assembly on the membrane surface).

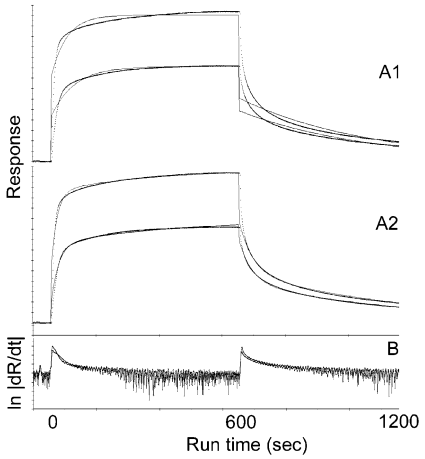


FIGURE 2: Comparison of the fit of one- and two-stage binding models for S1 binding to PC/PA membrane at two peptide concentrations. A1: Overlay plot of the experimental (dotted line) and calculated (solid line) sensorgrams using a 1:1 Langmuir model (lower plot, 0.75 $\mu$M; higher plot, 1.25 $\mu$M). A2: Same overlay plots but calculated using a two-stage model. B: Helper plot, logarithm of the absolute value of the slope of the sensorgrams as a function of time.

*(1) Data Analysis*. To obtain affinity constants of the interaction, the binding curves were first analyzed assuming a simple bimolecular association model. Panel A1 in Figure 2 shows sensorgrams of S1 binding to the PC/PA bilayer superimposed on the theoretical curves given by Biaevaluation 3.0 using a 1:1 Langmuir model. When this model is valid, the plot of the logarithm of the absolute value of the slope as a function of time for the association phase must be linear. Here, the ln |d$R$/d$t$| versus time plots were not linear (Figure 2, panel B), and the residuals (differences between measured and calculated curves) were high and not randomly distributed, indicating a poor fit of the sensorgrams to this model (as opposed to panel A2, which will be commented upon later). No mass transfer effects were observed as revealed by the unchanged kinetic constants at different flow rates (not shown). Both the concave shape of the ln |d$R$/d$t$| versus time plot and the poor fit of the binding curves to a 1:1 model imply the existence of a complex interaction between dermaseptins and the membrane bilayer. To test the existence of linked reactions, we examined the effect of contact time on dissociation rate. A high peptide concentration (2 $\mu$M) was injected for 2, 5, and 10 min, and the dissociation of the bound peptide was followed under buffer flow conditions. Figure 3 shows the outcome for dermaseptin S1. The dissociation rate was progressively slowed after longer injection times. The same behavior was observed for S4 (not shown). If reactions are independent and all binding sites are saturated, the dissociation rates are not influenced by contact time and therefore are identical. In our case, there is an increase in the stability of the peptide−membrane complex over time, which indicates the existence of linked reactions. There are three types of kinetically equivalent binding models for complex-linked reactions: bivalent analyte, heterogeneous analyte, and a two-stage reaction. The bivalent analyte reaction, which is used with analytes having two ligand-binding sites, such as antibody molecules, and the heterogeneous analyte reaction,

Table 2: Kinetic Rate Constants ($k_a$, $k_d$) and Affinity Constants ($K$) for the Interaction of Dermaseptins S1 and S4 with Lipid Bilayers of Two Different Compositions, Determined by Numerical Integration Using a Two-Stage Reaction Model

| | S1 | | S4 | |
|---|---|---|---|---|
| | PC | PC/PA | PC | PC/PA |
| $k_{a1}$ ($M^{-1}$ $s^{-1}$) | nd[e] | $2.8 \times 10^4$ ($\pm 0.7$)[a] | $3.3 \times 10^4$ ($\pm 2.6$) | $1.1 \times 10^3$ ($\pm 1.1$) |
| $k_{d1}$ ($s^{-1}$) | nd | $2.6 \times 10^{-2}$ ($\pm 0.9$) | $3.3 \times 10^{-2}$ ($\pm 3.0$) | $4.8 \times 10^{-4}$ ($\pm 1.0$) |
| $k_{a2}$ ($s^{-1}$) | nd | $2.0 \times 10^{-3}$ ($\pm 0.7$) | $2.6 \times 10^{-3}$ ($\pm 6.0$) | $8.5 \times 10^{-5}$ ($\pm 4.0$) |
| $k_{d2}$ ($s^{-1}$) | nd | $2.2 \times 10^{-3}$ ($\pm 0.4$) | $6.6 \times 10^{-4}$ ($\pm 1.5$) | $1.3 \times 10^{-5}$ ($\pm 17$) |
| $K_{app}$ ($M^{-1}$)[b] | $<7 \times 10^4$ | $9.9 \times 10^5$ | $4 \times 10^6$ | $1.5 \times 10^7$ |
| $K_{A1}$ ($M^{-1}$)[c] | nd | $1.1 \times 10^6$ | $1 \times 10^6$ | $2.3 \times 10^6$ |
| $K_{A2}$[d] | nd | 0.9 | 4 | 6.5 |

[a] Numbers in parentheses are the standard errors (SE) expressed as the percent of parameter values. [b] $(k_{a1}/k_{d1})(k_{a2}/k_{d2})$, apparent association affinity constant of the interaction. [c] $k_{a1}/k_{d1}$, association affinity constant of the first stage of the interaction. [d] $k_{a2}/k_{d2}$, association affinity constant of the second stage of the interaction. [e] nd, not determined.

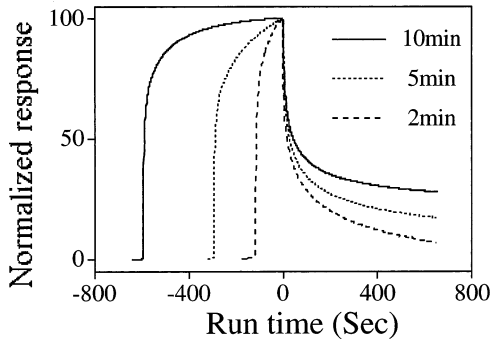


FIGURE 3: Effect of increased injection time on the stability of the peptide−membrane complex. Dermaseptin S1 was injected at 2 $\mu$M over the PC/PA bilayer for either 2, 5, or 10 min at a flow rate of 5 $\mu$L/min. Dissociation of the bound peptide in PBS buffer flow was recorded for 10 min.

which is intended for analysis of competing binding reactions that occur in a mixture of two analytes, seem to be very unlikely and can be ruled out. A two-stage reaction describes the binding process involving a conformational change that gradually leads to a more stable complex. This model may properly portray the interaction of antimicrobial peptides with lipid bilayers as a two-stage process composed of surface adhesion and membrane insertion stages. The insertion stage, taking place after the initial adhesion of the peptide to the membrane surface, may indicate a conformational change that occurs in the peptide−membrane complex and leads to increased stability of the complex.

*(2) Kinetic Analysis of the Dermaseptin−Membrane Interaction.* The entire data set was analyzed by a global fitting using a two-stage binding model. Panel A2 in Figure 2 shows the sensorgrams for S1 binding to PC/PA bilayer analyzed using the two-stage model. The calculations showed a good fit of experimental data to this model. The residuals were lower than the residuals obtained with a 1:1 model (Figure 2, panel A1), indicating a much better fit of the two-stage model for both the association and the dissociation phases. Table 2 summarizes the obtained kinetic rate constants and the derived affinity constants for the interaction of dermaseptins S1 and S4 with PC and PC/PA bilayers as determined using integrated equations of a two-stage model. The individual affinity constants of each stage of the interaction were calculated as the ratio of the respective association and dissociation rate constants. $K_{A1}$, the association affinity constant of the first stage of the interaction, indicates the peptides' affinity for adhesion to the membrane surface, whereas $K_{A2}$ is a unitless constant that reflects the peptides' tendency to insert into the membrane (efficacy of bilayer penetration by the peptide) and will be referred to as the insertion affinity. The apparent affinity constant for the global interaction, $K_A$, is a product of the individual affinity constants: $K_A = K_{A1}K_{A2}$.

For the sake of comparison, phosphatidylcholine and BSA were assayed under the same experimental conditions and found to have an affinity constant $K_{apparent}$ of $4.2 \times 10^{10}$ $M^{-1}$ and $<1 \times 10^3$ $M^{-1}$, respectively. Note also that the mathematical model used for calculating the rate constants assumes that the reactants are monomers in solution. Therefore, the affinity constants obtained for the aggregated peptides (S4 and to lesser extent $K_4K_{20}$-S4) can only be considered indicative.

We propose the following interpretation of the data shown in Table 2: The interaction of both peptides was stronger with anionic membranes. The absence of binding between dermaseptin S1 and the PC membrane at peptide concentrations of up to 1.5 $\mu$M indicated that the apparent affinity constant was lower than $7 \times 10^4$ $M^{-1}$ (the lowest detectable concentration is $0.1K_D$, where $K_D = 1/K_A$). As for the anionic membrane, S1 associated with PC/PA with a $k_{a1}$ value of $2.8 \times 10^4$ $M^{-1}$ $s^{-1}$ and dissociated with a $k_{d1}$ value of $2.6 \times 10^{-2}$ $s^{-1}$, giving the adhesion affinity $K_{A1}$ of $1.1 \times 10^6$ $M^{-1}$. After membrane adhesion, S1 inserted into the bilayer with a $k_{a2}$ value of $2.0 \times 10^{-3}$ $s^{-1}$ and "dissociated" (from the inserted form into the superficially adhering form) with a $k_{d2}$ value of $2.2 \times 10^{-3}$ $s^{-1}$, giving the insertion affinity $K_{A2}$ of 0.9. These individual affinity constants resulted in an apparent binding affinity of $9.9 \times 10^5$ $M^{-1}$. Compared with S1, therefore, dermaseptin S4 associated with PC/PA with 25-fold slower kinetics ($k_{a1} = 1.1 \times 10^3$ $M^{-1}$ $s^{-1}$), but the dissociation rate was 54-fold slower ($k_{d1} = 4.8 \times 10^{-4}$ $s^{-1}$), thus resulting in a 2-fold higher adhesion affinity ($K_{A1} = 2.3 \times 10^6$ $M^{-1}$). The kinetics of the second stage of the interaction was also much slower for dermaseptin S4, especially for the dissociation phase, resulting in a 7-fold higher insertion affinity ($K_{A2} = 6.5$) and in an overall 15-fold larger apparent binding affinity for S4 ($K_{app} = 1.5 \times 10^7$ $M^{-1}$). The slow off-rate of the second stage ($k_{d2}$) for S4 is at the lower end of the instrument range, where there is considerable error associated with its calculation because of the significant influence of even marginal baseline drift. Interestingly, the interaction of S4 with the zwitterionic PC bilayer proceeded with faster kinetics compared to PC/PA. Nevertheless, the calculated affinity constants demonstrated a 2-fold higher affinity for membrane adsorption and a 1.6-

Table 3: Kinetic Rate Constants for Dermaseptin S4 Derivatives Interacting with the PA/PC Bilayer, Determined by Numerical Integration Using a Two-Stage Reaction Model

| peptide | $k_{a1}$ ($10^3$ $M^{-1}$ $s^{-1}$) | $k_{d1}$ ($10^{-3}$ $s^{-1}$) | $k_{a2}$ ($10^{-4}$ $s^{-1}$) | $k_{d2}$ ($10^{-4}$ $s^{-1}$) |
|---|---|---|---|---|
| S4 | 1.1 (±1.1)[a] | 0.48 (±1.0) | 0.85 (±4.0) | 0.13 (±17) |
| $K_4K_{20}$-S4 | 23.9 (±2.0) | 26.2 (±2.7) | 38.8 (±2.3) | 2.23 (±2.9) |
| $K_4$-S4(1−16)a | 5.5 (±3.2) | 15.8 (±4.9) | 30.1 (±3.7) | 9.91 (±2.8) |
| $K_4$-S4(1−13)a | 2.42 (±2.8) | 20.3 (±1.7) | 14.1 (±3.9) | 15.6 (±2.0) |
| $K_4$-S4(1−10)a | 0.21 (±2.3) | 20.2 (±3.0) | 16.3 (±3.0) | 28.7 (±1.0) |

[a] Numbers in parentheses denote the standard error (SE) expressed as the percent of parameter values, which were based on measurements at five different concentrations in duplicates.

Table 4: Association Affinity Constants for Dermaseptins Binding to the PC/PA Bilayer, Compared with the Peptides' Cytolytic Activity against Human Erythrocytes and *Leishmania* Promastigotes

| peptide | $K_{adhesion}$ ($M^{-1}$) | $K_{insertion}$ | $K_{apparent}$ ($M^{-1}$) | $LC_{50}$ ($\mu$M)[a] | |
|---|---|---|---|---|---|
| | | | | RBC | *L. major* |
| S1 | $1.1 \times 10^6$ | 0.9 | $9.9 \times 10^5$ | 12 | 4.5 ± 1.5 |
| S4 | $2.3 \times 10^6$ | 6.5 | $1.5 \times 10^7$ | 1.4 ± 0.2 | 1.5 ± 0.5 |
| $K_4K_{20}$-S4 | $9.1 \times 10^5$ | 17.4 | $1.6 \times 10^7$ | 0.5 ± 0.1 | 1.5 |
| $K_4$-S4(1−16)a | $3.5 \times 10^5$ | 3.0 | $1.1 \times 10^6$ | 10 ± 0.5 | 6 |
| $K_4$-S4(1−13)a | $1.2 \times 10^5$ | 0.9 | $1.0 \times 10^5$ | 57 ± 3 | 9 ± 3 |
| $K_4$-S4(1−10)a | $1.0 \times 10^4$ | 0.6 | $6.0 \times 10^3$ | >100 | >50 |

[a] $LC_{50}$: peptide concentration producing 50% lysis of RBC or *Leishmania* promastigotes after 3 h of incubation (mean ± SD). $K_{adhesion}$ and $K_{insertion}$ represent the affinity constants of the first and second binding stages, respectively. Note: because of their aggregation state in solution (*14*) the affinity values of S4 and $K_4K_{20}$-S4 cannot be accurate and should be considered as indicative only.

fold higher affinity for membrane insertion in the case of the PC/PA bilayer, leading to a nearly 4-fold higher apparent affinity of S4 to the anionic membrane. However, as dermaseptin S4 forms aggregates in solution (*14*), these values should be considered as indicative only.

*Binding Properties of Dermaseptin S4 Derivatives.* To further challenge the Biacore system, we next determined the membrane-binding affinities of a series of dermaseptin S4 derivatives to the negatively charged bilayer (PC/PA) as described above and the binding data analyzed with the two-stage model. Table 3 presents the calculated kinetic rate constants of the interactions while Table 4 shows the derived affinity constants of the interactions, compared with the cytolytic activity of the peptides.

With the exception of the 10-mer derivative, all longer derivatives displayed faster kinetics than S4 for all stages of the interaction (Table 3). This probably reflects the significant hydrophobicity of the native peptide as expressed by its high apparent affinity for the phospholipid membrane. The insertion affinity value ($K_{insertion} = 6.5$) indicated that after the initial adhesion S4 has a high propensity to be incorporated within the bilayer. Addition of two positive charges to the native peptide further enhanced this propensity by nearly 3-fold increased insertion affinity ($K_{insertion} = 17.4$) even though the adhesion affinity was somewhat reduced. Compared with $K_4K_{20}$-S4, its C-terminal deletion derivative $K_4$-S4(1−16)a displayed a 3-fold reduced adhesion affinity and a 6-fold reduced insertion affinity, leading to an overall 15-fold decrease of apparent binding affinity ($1.1 \times 10^6$ $M^{-1}$). Further truncation of the peptide's C-terminus by another three residues resulted in another 3-fold loss of both adhesion and insertion affinities, leading to a 10-fold reduced apparent affinity ($1.0 \times 10^5$ $M^{-1}$). Finally, additional truncation of the peptide, down to 10 residues, led to further loss of apparent affinity by almost 2 orders of magnitude ($6 \times 10^3$ $M^{-1}$).

*Relationships between Membrane-Binding and Cytolytic Activity.* Human erythrocytes and *L. major* promastigotes were used as a more realistic model to the peptide−membrane interaction compared with PA/PC membrane, believing that cytolytic activity in other cell types may be governed by related properties. Our Biacore experiments describing the direct binding to the PC/PA membrane represent a fair simulation for peptide interaction with erythrocytes and *Leishmania* because of the exposed nature of their plasma membrane (as opposed to bacteria, for example) and the surface abundance of either phosphatidylcholine, which is the major component of the outer leaflet of erythrocyte membrane (*57*), or anionic lipophosphoglycans in the leishmanial membrane (*58*).

To understand the relationships between peptide binding to a membrane and the resulting cytotoxicity, binding parameters of the dermaseptin analogues were first compared with their hemolytic activity. The membrane-lytic activity was assessed by measuring the peptides' ability to induce hemoglobin leakage in PBS and is expressed as the peptide concentration that produced 50% hemolysis ($LC_{50}$). As shown in Table 4, a strong correlation was found between the peptides' apparent membrane affinity and their hemolytic activity. Thus, the hemolytic activity of S4 was increased by 3-fold after substitution of positions 4 and 20 with lysines, and in parallel, the apparent affinity also increased due to a 3-fold increase of the insertion affinity. Interestingly, despite its weaker hemolytic activity S4 adhered to the erythrocyte membrane more avidly than $K_4K_{20}$-S4, suggesting that higher surface binding does not necessary result in stronger cytolytic activity, which depends on the subsequent ability of the membrane-adsorbed peptide to be incorporated within the bilayer. Truncation of the peptide's C-terminus down to 16 and 13 residues, which resulted in progressive reduction of the apparent affinity, also led to a gradually reduced cytolytic activity. Finally, $K_4$-S4(1−10)a, which significantly lost the ability to bind and insert within the bilayer, became virtually unable to affect the integrity of the cell membrane.

Similar conclusions can be drawn from the interaction of these peptides with *L. major* promastigotes (Table 4).

*Peptide Orientation in the Membrane.* To verify the assumption that $K_{A2}$ yields information on the peptides' inserted state, we further characterized peptide binding to the RBC membrane. On the basis of the Biacore results, we selected two peptides, one highly hemolytic, $K_4K_{20}$-S4, and one weakly hemolytic, $K_4$-S4(1−13)a, that differ markedly (20-fold) in their insertion affinities (Table 4). If our postulation is correct, it requires that upon interaction with RBC $K_4$-S4(1−13)a should be significantly more susceptible

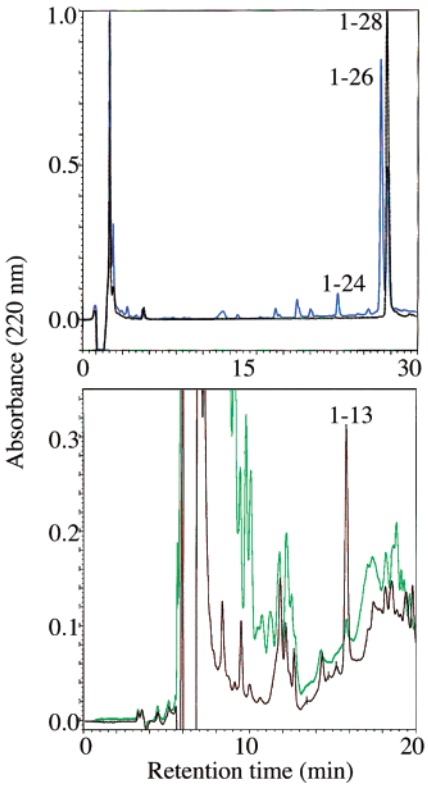


FIGURE 4: Evidence for superficial localization versus inserted state of dermaseptin derivatives. RBC were exposed to $K_4K_{20}$-S4 or to $K_4$-S4(1−13) at 10 $\mu$M each. Excess peptide was washed away, and peptide-bound RBC were exposed to proteinase K followed by extraction and HPLC analysis of the extracts. Relevant UV-absorbing peaks were identified by mass spectrometry. The upper panel shows overlay chromatograms of extracts from cells treated with $K_4K_{20}$-S4 in the presence (blue) and absence (black) of the proteolytic enzyme. In the presence of enzyme, $K_4K_{20}$-S4 (labeled 1−28) and two C-terminally truncated versions (labeled 1−26 and 1−24) were extracted, indicating that the peptide is predominantly protected but exposes slightly its C-terminal end. The lower panel shows the same for the 13-mer derivative in the presence (green) and absence (brown) of proteinase K. Less than 10% of the peptide was extracted in the presence of enzyme (labeled 1−13), indicating that the peptide is predominantly exposed (i.e., superficial localization). Note that $K_4K_{20}$-S4 extracts (upper panel) look "cleaner" since most cell constituents present in $K_4$-S4(1−13)-treated RBC were washed away after exposure to the hemolytic peptide.

to proteolysis than $K_4K_{20}$-S4 due to their respective positions on versus within the membrane. To test this assumption, RBC were allowed to interact with equimolar quantities of each peptide. After the incubation period, unbound peptide was washed away, and the peptide-bound RBC were exposed to the powerful proteolytic enzyme, proteinase K; then the membrane-bound peptides were extracted with a detergent and analyzed by HPLC. The identity of the extracted peptide was established by mass spectrometry analysis of the collected UV-absorbing HPLC peak (Figure 4). Extracts from untreated (no protease) samples showed that both peptides became membrane-bound after the incubation with RBC. Yet, the relative peak intensities revealed that $K_4K_{20}$-S4 bound to a much larger extent, reflecting a significantly higher apparent membrane affinity. After the proteolytic cleavage, only a small portion (<10%) of $K_4$-S4(1−13)a was recovered whereas nearly all of $K_4K_{20}$-S4 could be extracted either in its intact form or as shorter forms corresponding to truncation of the last two and four C-terminal residues. Expectedly, when the peptides were replaced by their D-amino acid isomers, the extracted quantities were similar to that of the L-isomers in the absence of proteinase K (not shown). Overall, these results demonstrate that, in agreement with the Biacore data, upon adhesion to the cell membrane, $K_4K_{20}$-S4 becomes deeply buried inside the hydrophobic core of the bilayer, whereas membrane-bound $K_4$-S4(1−13)a mostly remains in a superficial orientation.

## DISCUSSION

Biosensor technology was previously used to evaluate the membrane affinity of several antimicrobial peptides (*48*, *49*, *59*, *60*). The first study on cecropin peptides (*60*) was based on a simplifying assumption that the binding process proceeds by a simple bimolecular association between the peptide and the lipid (*61*). A later report on magainin and melittin interacting with lipid monolayers proposed that curve fitting with more complex algorithms including a two-stage binding and the parallel binding model yielded an improved fit (*48*). Here we examined the membrane-binding mechanism, particularly from the perspective of how binding data can be correlated with cytotoxicity. Our binding curves fitted well to a two-stage interaction model. A two-state model of action of antimicrobial peptides (*32*) supports such a binding mechanism. We find that the Biacore two-stage model enables dissection of the binding process into two distinct components, each of which describing individual steps of the interaction. This allows us not only to distinguish between peptides according to their membrane affinity ($K_{app}$) but also to characterize them by their behavior at different steps of the interaction with the membrane, namely, by elucidating the adhesion ($K_1$ or $K_{adhesion}$) and insertion ($K_2$ or $K_{insertion}$) affinity constants.

Note that a similar conclusion was drawn from isothermal titration calorimetry (ITC), where $K_{insertion}$ was referred to as the intrinsic (hydrophobic) partition coefficient. Coefficients were calculated for various cationic peptides using the Gouy−Chapman theory (correcting for electrostatic effects) in combination with surface partition equilibrium (*62*, *63*).

According to the two-state model (*32*) the insertion step is concentration-dependent and occurs when a critical (threshold) concentration of the membrane-bound peptide is reached. Assembly of surface-adsorbed monomers is believed to be required for a subsequent membrane permeabilization activity. Peptides that do not assemble are randomly distributed on the membrane surface, are unable to insert within the bilayer, and consequently are unable to permeabilize the cell. Such a "naive" binding was observed, for instance, with nonaggregating dermaseptin S4 derivatives, S4(9−28) or $K_4$-S4(1−13)a (*14*, *46*). These peptides were shown to bind rather avidly to the membrane of model liposomes or cells but did not cause cell destruction, demonstrating that binding of antimicrobial peptides to the cell membrane does not necessarily lead to cytotoxicity. $K_2$ may indicate, therefore, not only the peptides' tendency to insert into the membrane but also their ability to assemble within the membrane and subsequently transit from the surface state to the insertion state, which leads to membrane permeabilization.

In accordance with previous data (*19*, *45*) dermaseptins S1 and S4 interacted preferentially with acidic phospholipids,

reflecting the importance of electrostatic interactions in the binding process. The calculated affinity constants (Table 2) appear biologically reasonable and similar to the values found for magainin and melittin binding to zwitterionic and anionic membranes (*48*, *49*). S4 possessed higher adhesion and higher insertion affinity than S1 to both kinds of membranes, probably due to higher positive charge (four versus three) and larger hydrophobicity of S4 compared with S1 (*36*). The calculated insertion affinities showed that dermaseptin S4 was highly efficient in penetrating into both the PC and PC/PA bilayers, whereas dermaseptin S1 was able to insert slightly into PC/PA but was virtually unable to interact with the PC membrane. These results are in good agreement with previous fluorescence-based studies in which S1 was shown to undergo some self-assembly on the surface of acidic but not zwitterionic vesicles and to undergo a shallow penetration into acidic membranes only (*19*) whereas S4 was found to insert into both acidic and zwitterionic vesicles (*45*).

Similarly, S4 interaction kinetics with membranes was proposed to be slow (*45*), as confirmed here. This fact is probably related to its high aggregation state already in solution and the time it takes for the tight aggregate to dissociate, thus resulting in a prolonged mode of association (Figure 1). Accordingly, inhibition of the aggregation state in $K_4K_{20}$-S4 led to increased interaction kinetics. $K_4K_{20}$-S4 displayed somewhat lower adhesion affinity than S4 but was significantly more potent in membrane penetration and in cytotoxicity. Although this could reflect inaccurate determination of the affinity constants of these peptides (because of their aggregated states in solution), it could also mean that the tight S4 aggregate is more avidly associated with the membrane than the less aggregated $K_4K_{20}$-S4 due to a more efficient hydrophobic interaction of the aggregate. On the other hand, after rapid surface binding of the higher charged $K_4K_{20}$-S4, negatively charged phospholipid groups of PC/PA could neutralize the electrostatic repulsions between peptide monomers and promote peptide assembly within the membrane, resulting in a more efficient permeabilization activity.

Proteolytic cleavage experiments supported the Biacore data concerning the effectiveness of membrane penetration. $K_4K_{20}$-S4 was substantially protected from proteolytic treatment, whereas $K_4$-S4(1−13)a, which displayed a 20-fold lower insertion affinity, was much more susceptible to proteolysis, suggesting a more superficial localization. In accordance with these considerations, a correlation was found between the apparent membrane affinity of the peptides and their membranolytic activity, namely, the more lytic peptides possessing a higher apparent affinity. A high adhesion affinity is generally required for potent cytotoxicity, but it is not enough; the insertion affinity is apparently a major component of the lytic activity. Thus, despite possessing a lower adhesion affinity than S1 or S4, the derivative $K_4K_{20}$-S4 exhibited the highest lytic potency because of its highest insertion affinity (Table 4). The surface state is functionally inactive, and binding will lead to cell lysis only if the adsorbed peptides have sufficient insertion affinity (this may require the ability to undergo surface oligomerization); otherwise, it remains a naive binding, such as the strong but nontoxic binding of S4(13−28) or $K_4$-S4(1−13)a to human erythrocytes. This superficial localization, nonetheless, can be put to advantage as described (*46*).

In conclusion, the present study confirmed that the biosensor technology using a lipid bilayer is a powerful system for investigations of peptide−membrane interactions and that a two-stage model is a reliable algorithm for data analysis that allows qualitative and quantitative comparisons between closely related analogues. More importantly, our results suggest that the system can be exploited for the selection of designed molecules with the desired membrane-binding properties, either molecules with a high membrane penetrating ability or molecules that merely strongly adhere to the membrane.

## REFERENCES


1. Travis, J. (1994) *Science 264*, 360−362.
2. Gold, H. S., and Moellering, R. C. (1996) *N. Engl. J. Med. 335*, 1445−1453.
3. Nicolas, P., and Mor, A. (1995) *Annu. Rev. Immunol. 49*, 277−304.
4. Boman, H. G. (1995) *Annu. Rev. Immunol. 13*, 61−92.
5. Mor, A. (2001) *The Kirk-Othmer Encyclopedia of Chemical Technology*, John Wiley & Sons, New York (http://www3.interscience.wiley.com: 8095/articles/peptwise.a01/frame.html).
6. Zasloff, M. (2002) *Nature 415*, 389−395.
7. Levy, O. (2000) *Blood 96*, 2664−2672.
8. Hancock, R. E., and Lehrer, R. (1998) *Trends Biotechnol. 16*, 82−90.
9. Ganz, T., and Lehrer, R. (1998) *Curr. Opin. Immunol. 10*, 41−44.
10. Andreu, D., and Rivas, L. (1998) *Biopolymers 47*, 415−433.
11. Tossi, A., Sandri, L., and Giangaspero, A. (2000) *Biopolymers 55*, 4−30.
12. Maloy, L. W., and Kari, U. P. (1995) *Biopolymers 37*, 105−122.
13. Blondelle, E. S., and Lohner, K. (2000) *Biopolymers 55*, 74−87.
14. Kustanovich, I., Shalev, D. E., Mikhlin, M., Gaidukov, L., and Mor, A. (2002) *J. Biol. Chem. 277*, 16941−16951.
15. Shai, Y. (1999) *Biochim. Biophys. Acta 1462*, 55−70.
16. Shai, Y. (2002) *Biopolymers 66*, 236−248.
17. Ladokhin, A. S., Selsted, M. E., and White, S. H. (1997) *Biophys. J. 72*, 1762−1766.
18. Gazit, E., Boman, A., Boman, H. G., and Shai, Y. (1995) *Biochemistry 34*, 11479−11488.
19. Pouny, Y., Rapaport, D., Mor, A., Nicolas, P., and Shai, Y. (1992) *J. Biol. Chem. 31*, 12416−12423.
20. Strahilevitz, J., Mor, A., Nicolas, P., and Shai, Y. (1994) *J. Biol. Chem. 33*, 10951−10960.
21. Moll, G. N., Brul, S., Konings, W. N., and Driessen, A. J. (2000) *Biochemistry 39*, 11907−11912.
22. Oren, Z., and Shai, Y. (2000) *Biochemistry 39*, 6103−6114.
23. Friedrich, C. L., Moyles, D., Beveridge, T. J., and Hancock, R. E. (2000) *Antimicrob. Agents Chemother. 44*, 2086−2092.
24. Sokolov, Y., Mirzabekov, T., Martin, D. W., Lehrer, R. I., and Kagan, B. L. (1999) *Biochim. Biophys. Acta 1420*, 23−29.
25. Duclohier, H., and Wroblewski, H. (2001) *J. Membr. Biol. 184*, 1−12.
26. Matsuzaki, K., Murase, O., Fujii, N., and Miyajima, K. (1995) *Biochemistry 34*, 6521−6526.
27. Ammar, B., Perianin, A., Mor, A., Sarfati, G., Tissot, M., Nicolas, P., Giroud, J. P., and Arveiller, M. (1998) *Biochem. Biophys. Res. Commun. 247*, 870−875.
28. Hariton, E., Fineberg, K., Feder, R., Mor, A., Graessmann, A., Brack-Werner, R., Gilon, C., and Loyter, A. (2002) *Biochemistry 41*, 9208−9214.
29. Scott, M. G., Rosenberger, C. M., Gold, M. R., Finlay, B. B., and Hancock, R. E. (2000) *J. Immunol. 165*, 3358−3365.
30. Ludtke, S. J., He, K., Wu, Y., and Huang, H. W. (1994) *Biochim. Biophys. Acta 1190*, 181−184.
31. Heller, W. T., Waring, A. J., Lehrer, R. I., and Huang, H. W. (1998) *Biochemistry 37*, 17331−17338.
32. Huang, H. W. (2000) *Biochemistry 39*, 8347−8352.
33. Mor, A., Nguyen, V. H., Delfour, A., Migliore, S. D., and Nicolas, P. (1991) *Biochemistry 30*, 8824−8830.
34. Mor, A., and Nicolas, P. (1994) *Eur. J. Biochem. 219*, 145−154.
35. Mor, A., Amiche, M., and Nicolas, P. (1994) *Biochemistry 33*, 6642−6650.

36. Mor, A., Hani, K., and Nicolas, P. (1994) *J. Biol. Chem. 269*, 31635−31640.
37. Hernandez, C., Mor, A., Dagger, F., Nicolas, P., Hernandez, A., Benedetti, E. L., and Dunia, I. (1992) *Eur. J. Cell Biol. 59*, 414−424.
38. Mor, A., Nguyen, V. H., and Nicolas, P. (1991) *J. Mycol. Med. 1*, 5−10.
39. DeLucca, A. J., Bland, J. M., Jacks, T. J., Grimm, C., and Walsh, T. J. (1998) *Med. Mycol. 36*, 291−298.
40. Mor, A., and Nicolas, P. (1994) *J. Biol. Chem. 269*, 1934−1939.
41. Coot, P. J., Holyoak, C. D., Bracey, D., Ferdinando, D. P., and Pearce, J. A. (1998) *Antimicrob. Agents Chemother. 42*, 2160−2170.
42. Feder, R., Dagan, A., and Mor, A. (2000) *J. Biol. Chem. 275*, 4230−4238.
43. Krugliak, M., Feder, R., Zolotarev, V. Y., Gaidukov, L., Dagan, A., Ginsburg, H., and Mor, A. (2000) *Antimicrob. Agents Chemother. 44*, 2442−2451.
44. Dagan, A., Efron, L., Gaidukov, L., Mor, A., and Ginsburg, H. (2002) *Antimicrob. Agents Chemother. 46*, 1059−1066.
45. Ghosh, J. K., Shaool, D., Guillaud, P., Ciceron, L., Mazier, D., Kustanovich, I., Shai, Y., and Mor, A. (1997) *J. Biol. Chem. 272*, 31609−31616.
46. Feder, R., Nehushtai, R., and Mor, A. (2001) *Peptides 22*, 1683−1690.
47. Navon-Venezia, S., Feder, R., Gaidukov, L., Carmeli, Y., and Mor, A. (2002) *Antimicrob. Agents Chemother. 46*, 689−694.
48. Mozsolilits, H., Wirth, H. J., Werkmeister, J., and Aguilar, M. I. (2001) *Biochim. Biophys. Acta 1512*, 64−76.
49. Papo, N., and Shai, Y. (2003) *Biochemistry 42*, 458−466.
50. MacDonald, R. C., MacDonald, R. I., Menco, B. P., Takeshita, K., Subbarao, N. K., and Hu, L. R. (1991) *Biochim. Biophys. Acta 1061*, 297−303.
51. Jönsson, U., Fägerstam, L., Ivarsson, B., Johnsson, B., Karlsson, R., Lundh, K., Löfås, S., Persson, B., Roos, H., Rönnberg, I., Sjölander, S., Stenberg, E., Ståhlberg, R., Urbaniczky, C., Östlin, H., and Malmqvist, M. (1991) *BioTechniques 11*, 620−627.
52. Cooper, M. A., Hansson, A., Löfås, S., and Williams, D. H. (2000) *Anal. Biochem. 277*, 196−205.
53. Cooper, M. A., Try, A. C., Carroll, J., Ellar, D. J., and Williams, D. H. (1998) *Biochim. Biophys. Acta 1373*, 101−111.
54. Morton, T. A., Miszka, D. G., and Chaiken, I. M. (1995) *Anal. Biochem. 227*, 176−185.
55. O'Shanessy, D. J., Brigham-Burke, M., Soneson, K. K., and Hensley, P. (1993) *Anal. Biochem. 212*, 457−468.
56. Karlsson, R., and Fault, A. (1997) *J. Immunol. Methods 200*, 121−133.
57. Opden-Kamp, J. A. F. (1979) *Anal. Rev. Biochem. 48*, 47−71.
58. Turco, S. J., and Descoteaux, A. (1992) *Anal. Rev. Microbiol. 46*, 65−94.
59. Blondelle, S. E., Lohner, K., and Aguilar, M. I. (1999) *Biochim. Biophys. Acta 1462*, 89−108.
60. Wang, W., Smith, D. K., Moulding, K., and Chen, H. M. (1998) *J. Biol. Chem. 273*, 27438−27448.
61. Ben-Tal, N., Honig, B., Peitzsch, R. M., Denisov, G., and McLaughlin, S. (1997) *Biophys. J. 71*, 561−575.
62. Wenk, M. R., and Seelig, J. (1998) *Biochemistry 37*, 3909−3916.
63. Wieprecht, T., Beyermann, M., and Seelig, J. (1999) *Biochemistry 38*, 10377−10387.
64. *Kinetic and Affinity Analysis using BIA* (1998) Biacore AB, Uppsala, Sweden.

BI034514X